A Variational Method for Expanding the Bit-Depth of Low Contrast Image

Motong Qiao, Wei Wang, and Michael K. Ng

Department of Mathematics, Hong Kong Baptist University

Abstract. Traditionally, bit-depth expansion is an image processing technique to display a low bit-depth image on a high bit-depth monitor. In this paper, we study a variational method for expanding the bit-depth of low contrast images. Our idea is to develop a variational approach containing an energy functional to determine a local mapping function $f(r, x)$ for bit-depth expansion via a smoothing technique, such that each pixel can be adjusted locally to a high bit-depth value. In order to enhance low contrast images, we make use of the histogram equalization technique for such local mapping function. Both bit-depth expansion and equalization terms can be combined together into the resulting objective function. In order to minimize the differences among the local mapping function at the nearby pixel locations, the spatial regularization of the mapping is incorporated in the objective function. Experimental results are reported to show that the performance of the proposed method is competitive with the other compared methods for several testing low contrast images.

Keywords: bit-depth expansion, variational methods, low contrast, spatial regularization.

1 Introduction

The bit-depth of an image refer to the number of bits used to represent a pixel value. A high bit-depth implies greater ability to store the information. The most widely used images are 8-bit in gray-level or 24-bit in color, which are suitable for displaying on traditional Cathode Ray Tube (CRT) monitors. There are some legacy images stored in a low bit-depth. Also high bit-depth images are emerging along with the development of capturing and displaying instruments in imaging sciences. A low bit-depth image has its advantages on saving storage space and transmission. However, content and contrast are distorted in low bit-depth images. In particular, it would be useful and interesting to display a high bit-depth image from a low bit-depth and low contrast image and This paper aims at investigating an variational method to expand the bit-depth of low contrast images.

1.1 Bit-Depth Expansion Methods

The conventional methods for bit-depth expansion include zero-padding (ZP), multiplication-by-an-ideal-gain (MIG) [1], bit-replication (BR) [1], Gamma-expansion (GE) [2], and high dynamic range imaging (HDRI). Whereas HDRI

A. Heyden et al. (Eds.): EMMCVPR 2013, LNCS 8081, pp. 54–65, 2013.

usually requires a collection of photographs taken with different exposures, for instance the methods in [3–6], we focus on the problem of expanding the bit-depth from one given image only.

The bit-depth expansion problem came up from the inverse image dithering problem. The problem can be depicted as follows. Given a $p-$bit image X with a range $[0, 2^p - 1]$ and a $q-$bit $(q > p)$ image Y with a range $[0, 2^q - 1]$, the goal is to convert X to Y. Obviously the most simple idea is through zero padding (ZP): $[Y]_{i,j} = [X]_{i,j} \times 2^{(q-p)}$. Another basic method is to multiply an ideal gain (MIG) and then round to the nearest integer:

$$[Y]_{i,j} = \text{Round}\left([X]_{i,j} \times \frac{2^q - 1}{2^p - 1}\right)$$

The other method combining the gamma selection is used in Akyuz's psychophysical experiments [2], namely gamma expansion (GE) method:

$$Y = k(\frac{X - X_{\min}}{X_{\max} - X_{\min}})^{\gamma},$$

where k represents the highest possible value of Y and γ determines the nonlinearity of the scaling. In [1], a bit replication (BR) method is proposed:

$$[X]_{i,j} = x_{p-1}x_{p-2}\cdots x_1x_0; \quad [Y]_{i,j} = x_{p-1}x_{p-2}\cdots x_1x_0x_{p-1}x_{p-2}\cdots,$$

where x_k is the k^th bit of the (i, j)th pixel value $[X]_{i,j}$ of X. These methods achieve an one-to-one mapping, which means a gray level in a low bit-depth image can only be mapped to a certain gray level in a high bit-depth image. It is clear that these methods do not consider spatial pixel locations in adjusting pixel values. Thus the resulting image may suffer from contouring artifacts. Recently, a more sophisticated method is proposed in [7]. The idea is to use MIG as initialization of the high bit-depth image, and then remove the contouring artifacts by a spatial variant filter based on the segmentation of the contour suffered region. The results of this two-step method depend on whether the contour region can be correctly divided from smooth regions. In [8], other low-pass filters with adaptive windows size are developed to obtain a better performance in edge-preservation and contour removal.

1.2 The Contribution

In this paper, we propose and develop a variational approach containing an energy functional to determine a local mapping function $f(r, x)$ for bit-depth expansion, such that each pixel can be adjusted locally to a high bit-depth value. Here r refers to the variable for the number of bits used and x refers to the variable for pixel locations. A smoothing technique can be employed in the expansion process by considering the regularization based on the first-order derivative of f with respect to r: $\int_x \int_r f_r(r, x)^2$. Since low bit-depth images may be degraded due to exposure reasons [9], the visual appearance (contrast) of the

displayed image should be enhanced in the variational method. We can make use of the histogram equalization technique to find a local mapping function to enhance low contrast images: $\int_x \int_r f_r(r,x)^2/h(r,x)$ where $h(r,x)$ is the local histogram of a low contrast image. As both bit-expansion and histogram equalization processes involves the first-order derivative of f with respect to r, we combine them together into the resulting objective function. In order to minimize the differences among the local mapping function at the nearby pixel locations, the spatial regularization of the mapping is also incorporated in the functional: $\int_x \int_r \|\nabla f(r,x)\|_2^2$. To adjust a local mapping function, we also incorporate another penalty term to require the mean brightness of the displayed image can be close to that of the input image. Experimental results are reported to show that the performance of the proposed method is competitive with the other compared methods for several testing low contrast images.

The outline of this paper is organized as follows. In Section 2, we will describe the proposed model. In Section 3, we will present the algorithm to solve the proposed model numerically. In Section 4, we will present numerical examples to show the effectiveness of the proposed model. Finally, the concluding remarks will be given in Section 5.

2 The Proposed Model

Our main idea is to make use of histogram equalization and smoothing techniques to determine an local mapping function to display low bit-depth and low contrast images. Let r and s represent the normalized variables for a low contrast low bit-depth image and its displayed bit-expanded image respectively, i.e., $0 \leq r, s \leq 1$. Assume that $h(r)$ represents the normalized histograms for the input low bit-depth image. A function $s = f(r)$, is used to map each input level r to a new level s to achieve the required enhancement objective. It has been shown in [10] that the histogram equalization problem can be considered a variational minimization problem as follows:

$$\min_f J(f) = \int_0^1 \frac{1}{h(r)} f_r^2 \mathrm{dr}, \tag{1}$$

where f_r is the first derivative of f with respect to r.

Suppose Ω denotes the image domain. In order to preserve more local image details and to make the enhancement according to such details of an input low bit-depth image, we employ a local transformation $f(r,x)$, where $(r,x) \in \Lambda = (0,1) \times \Omega$. Here, at each pixel location x, we design a transformation $f(r,x)$. Then a term of an objective function should contain

$$\int_\Lambda \frac{1}{h(r,x)} f_r(r,x)^2 \mathrm{dxdr}. \tag{2}$$

On the other hand, a smoothing technique is used for bit-depth expansion. We can include a term

$$\int_\Lambda f_r(r,x)^2 \mathrm{dxdr}$$

Here $f_r(r,x)$ is the first-order derivative of f with respect to r. As both bit-expansion and histogram equalization processes involves $f_r(r,x)$, we combine them together by considering (2) only into the resulting objective function.

In order to minimize the differences among the local transformations at the nearby pixel locations, the spatial regularization of the transformation is also incorporated in the functional for the equalization process. In particular, we consider the H_1-norm regularization $|\nabla f|^2$ of f in the model, where ∇ denotes the gradient operator of f with respect to the horizontal and vertical directions of an image. Moreover, we can incorporate another penalty term that the mean brightness of the displayed high bit-depth image can be close to that of the input low bit-depth image. The proposed variational model is given as follows:

$$\Phi(f) = \int_\Lambda \frac{1}{h(r,x)} f_r(r,x)^2 \mathrm{dxdr} + \gamma_1 \int_\Lambda |\nabla f|^2 \mathrm{dxdr} + \gamma_2 \int_\Omega \left(\int_0^1 f h(r,x) \mathrm{dr} - \mu \right)^2 \mathrm{dx}, \tag{3}$$

where γ_1 and γ_2 are two positive regularization parameters, and μ is the mean brightness of the input low bit-depth image.

According to [7, 8], the disadvantage of ZP, MIG, BR and GE methods is that they only provide one-to-one mapping from a low to high bit-depth image. Indeed, most of possible values in high bit-depth image are not used. In the proposed, we make use of the variational method to determine a local transformation which gives a one-to-many mapping from a low to high bit-depth image. According to local transformation based on local image details, the same pixel value at two different locations may be mapped to two different pixel values, and the two pixel values at the nearby pixel locations may be mapped to close pixel values. We expect the noise and contour artifacts of the displayed high bit-depth image can be resolved, and its local contrast can also be enhanced.

In a discrete setting, the functional in (3) can be written as follows:

$$\Phi_d(\mathbf{f}) = \sum_{i=1}^{R} \sum_{j=1}^{N} \frac{(\mathbf{D}_{i,j}^{(r)} \mathbf{f})^2}{h_{i,j}} + \gamma_1 \sum_{i=1}^{R} \sum_{j=1}^{N} \left\| \mathbf{D}_{i,j}^{(x)} \mathbf{f} \right\|_2^2 + \gamma_2 \sum_{j=1}^{N} \left(\sum_{i=1}^{R} \mathbf{f}_{i,j} h_{i,j} - \mu \right)^2, \tag{4}$$

where R and N refers to the number of high bit-depth levels and the number of pixel values respectively, $\mathbf{f} = [\mathbf{f}_{i,j}]$ is the n-vector containing the transformation function values at the i-th high bit-depth level and j-th pixel location (the lexicographic ordering of $\mathbf{f}$ is used), $n = R \times N$ refers to the total number of unknowns. For a displayed high bit-depth image of q bits, R is equal to 2^q. Moreover, $\mathbf{D}_{i,j}^{(r)} \mathbf{f}$ is the discrete derivative value of $\mathbf{f}$ with respect to the i-th high bit-depth level at j-th pixel location, and $\mathbf{D}_{i,j}^{(x)} \mathbf{f}$ is the discrete gradient vector of $\mathbf{f}$ with respect to the j-th pixel location at the i-th high bit-depth level (the Euclidean norm $\|\mathbf{D}_{i,j}^{(x)} \mathbf{f}\|_2^2$ is used). It is clear that $\mathbf{D}_{i,j}^{(r)}$ is an 1-by-n matrix and $\mathbf{D}_{i,j}^{(x)}$ is an 2-by-n matrix for $1 \le i \le R$ and $1 \le j \le N$.

As a summary, the following minimization problem is employed for displaying a high bit-depth image:

$$\min_{\mathbf{f}} \Phi_d(\mathbf{f}) \quad \text{subject to } 0 \le \mathbf{f} \le 1 \tag{5}$$

3 The Algorithm

In practice, we employ the alternating direction method of multipliers (ADMM) to solve the constrained optimization problem in (5). For simplicity, we form n-by-n matrix $\mathbf{D}^{(r)} = [(\mathbf{D}_{i,j}^{(r)})^T]$ and $2n$-by-n matrix $\mathbf{D}^{(x)} = [(\mathbf{D}_{i,j}^{(x)})^T]$. By using the Lagrangian multipliers λ_1, λ_2, λ_3, λ_4 to the linear constraints:

$$\mathbf{u} = \mathbf{D}^{(r)}\mathbf{f}, \quad \text{and} \quad \mathbf{v} = \mathbf{w} = \mathbf{z} = \mathbf{f},$$

with $\mathbf{u} = [u_{i,j}]$, the augmented Lagrangian function is given by

$$\begin{aligned}
&\mathcal{L}(\mathbf{f}, \mathbf{u}, \mathbf{v}, \mathbf{w}, \mathbf{z}, \lambda_1, \lambda_2, \lambda_3, \lambda_4) \\
&= \iota(\mathbf{z}) + \sum_{i=1}^{R}\sum_{j=1}^{N} \frac{\mathbf{u}_{i,j}^2}{h_{i,j}} + \gamma_1 \sum_{i=1}^{R}\sum_{j=1}^{N} \left\| \mathbf{D}_{i,j}^{(x)}\mathbf{v} \right\|_2^2 + \gamma_2 \sum_{j=1}^{N} \left(\sum_{i=1}^{R} \mathbf{w}_{i,j} h_{i,j} - \mu \right)^2 + \\
&< \lambda_1, \mathbf{u} - \mathbf{D}^{(r)}\mathbf{f} > + < \lambda_2, \mathbf{v} - \mathbf{f} > + < \lambda_3, \mathbf{w} - \mathbf{f} > + < \lambda_4, \mathbf{z} - \mathbf{f} > + \\
&\beta(||\mathbf{u} - \mathbf{D}^{(r)}\mathbf{f}||_2^2 + ||\mathbf{v} - \mathbf{f}||_2^2 + ||\mathbf{w} - \mathbf{f}||_2^2 + ||\mathbf{z} - \mathbf{f}||_2^2),
\end{aligned}$$

where

$$\iota(\mathbf{z}) := \begin{cases} 0, & 0 \le \mathbf{z} \le 1, \\ +\infty, & \text{otherwise}, \end{cases}$$

and $< \cdot, \cdot >$ is the inner product of Euclidean space.

The Algorithm:

(i) Set $\mathbf{f}^0 = \tilde{\mathbf{f}}$, $\lambda_1^0 = \tilde{\lambda}_1$, $\lambda_2^0 = \tilde{\lambda}_2$, $\lambda_3^0 = \tilde{\lambda}_3$, $\lambda_4^0 = \tilde{\lambda}_4$ be the initial input data;

(ii) At the kth iteration:

– Given $\mathbf{f}^k$, λ_1^k, λ_2^k, λ_3^k, λ_4^k, and compute $\mathbf{u}^{k+1}$, $\mathbf{v}^{k+1}$, $\mathbf{w}^{k+1}$, $\mathbf{z}^{k+1}$ by solving:

$$\min_{\mathbf{u},\mathbf{v},\mathbf{w},\mathbf{z}} \mathcal{L}(\mathbf{f}^k, \mathbf{u}, \mathbf{v}, \mathbf{w}, \mathbf{z}, \lambda_1^k, \lambda_2^k, \lambda_3^k, \lambda_4^k); \tag{6}$$

– Given $\mathbf{u}^{k+1}, \mathbf{v}^{k+1}, \mathbf{w}^{k+1}, \mathbf{z}^{k+1}$, and compute $\mathbf{f}^{k+1}$ by solving:

$$\mathcal{L}(\mathbf{f}, \mathbf{u}^{k+1}, \mathbf{v}^{k+1}, \mathbf{w}^{k+1}, \mathbf{z}^{k+1}, \lambda_1^k, \lambda_2^k, \lambda_3^k, \lambda_4^k); \tag{7}$$

– Updating $\lambda_1^{k+1}, \lambda_2^{k+1}, \lambda_3^{k+1}, \lambda_4^{k+1}$ by using:

$$\begin{aligned}
\lambda_1^{k+1} &= \lambda_1^k + 2 * \beta(\mathbf{u}^{k+1} - \mathbf{D}^{(r)}\mathbf{f}^{k+1}), \\
\lambda_2^{k+1} &= \lambda_2^k + 2 * \beta(\mathbf{v}^{k+1} - \mathbf{f}^{k+1}), \\
\lambda_3^{k+1} &= \lambda_3^k + 2 * \beta(\mathbf{w}^{k+1} - \mathbf{f}^{k+1}), \\
\lambda_4^{k+1} &= \lambda_4^k + 2 * \beta(\mathbf{z}^{k+1} - \mathbf{f}^{k+1}).
\end{aligned}$$

(iii) Go back to Step (ii) until $\frac{||\mathbf{f}^{k+1} - \mathbf{f}^k||}{||\mathbf{f}^{k+1}||} \leq \epsilon$.

For the subproblem in (6), all the unknowns can be solved separately. In the next section, we test the proposed algorithm to expand low bit-depth and low contrast images.

4 Numerical Results

For ease and obviousness of displaying the results, we test our variational method on 8-bit (in each channel) RGB images of size 256×256 as shown in Figures 1-5(a). The input images in Figures 1-5(b) are obtained from 8-bit original images in Figures 1-5(a) by averaging, and some of them are manually lowered the contrast

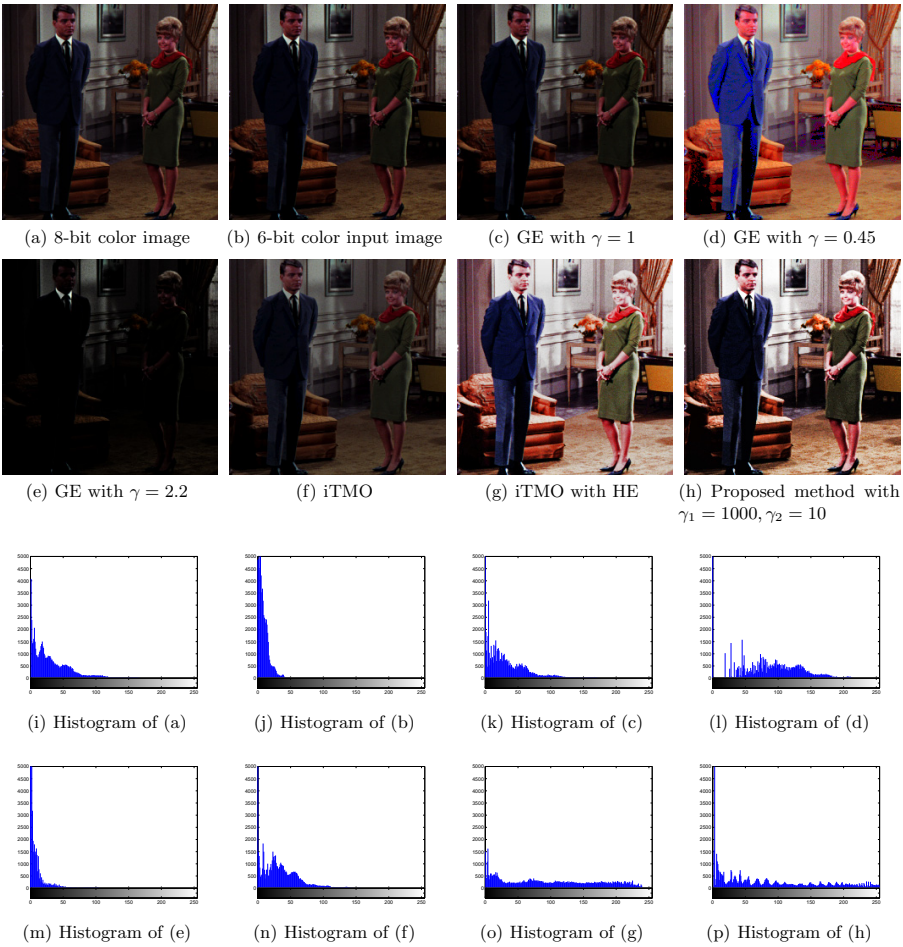

(a) 8-bit color image (b) 6-bit color input image (c) GE with $\gamma = 1$ (d) GE with $\gamma = 0.45$

(e) GE with $\gamma = 2.2$ (f) iTMO (g) iTMO with HE (h) Proposed method with $\gamma_1 = 1000, \gamma_2 = 10$

(i) Histogram of (a) (j) Histogram of (b) (k) Histogram of (c) (l) Histogram of (d)

(m) Histogram of (e) (n) Histogram of (f) (o) Histogram of (g) (p) Histogram of (h)

Fig. 1. The Comparison of different methods for the "Couple" image

Table 1. PSNR value comparison

Input	PSNR (dB)					
Images	Proposed	GE with $\gamma = 1$	GE with $\gamma = 0.45$	GE with $\gamma = 2.2$	iTMO	iTMO with HE
Lena	**19.49**	19.09	9.66	6.65	17.09	17.46
Boats	20.22	20.17	13.13	7.53	17.56	**20.42**
Monolake	**24.33**	9.24	12.14	10.23	12.03	20.23
Peppers	**29.35**	7.13	10.09	17.17	9.84	19.22

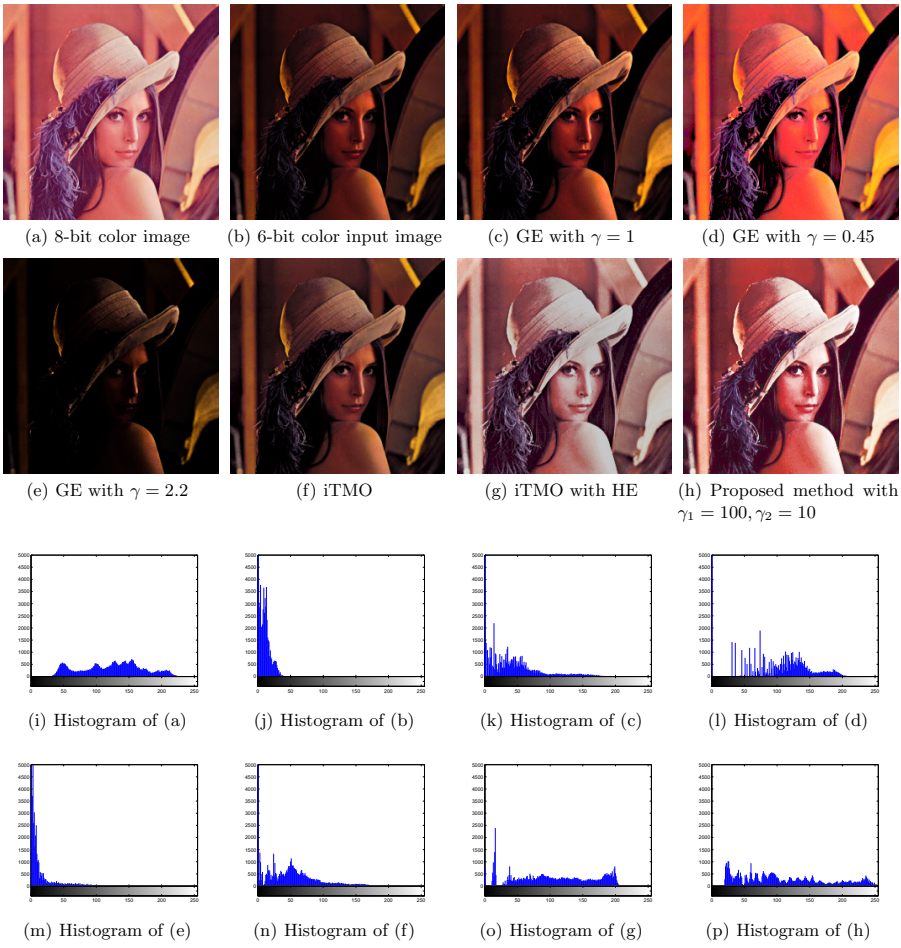

(a) 8-bit color image (b) 6-bit color input image (c) GE with $\gamma = 1$ (d) GE with $\gamma = 0.45$

(e) GE with $\gamma = 2.2$ (f) iTMO (g) iTMO with HE (h) Proposed method with $\gamma_1 = 100, \gamma_2 = 10$

(i) Histogram of (a) (j) Histogram of (b) (k) Histogram of (c) (l) Histogram of (d)

(m) Histogram of (e) (n) Histogram of (f) (o) Histogram of (g) (p) Histogram of (h)

Fig. 2. The Comparison of different methods for the "Lena" image

or biased the exposure to simulate different degradation cases. We see from Figures 1(h)-(i), the histogram are biased toward the small values, and this input image in is underexposed. Here the histogram combines all the pixel values in the red, green and blue channels. We see from Figures 2-5(h) that the histograms of Figures 2-

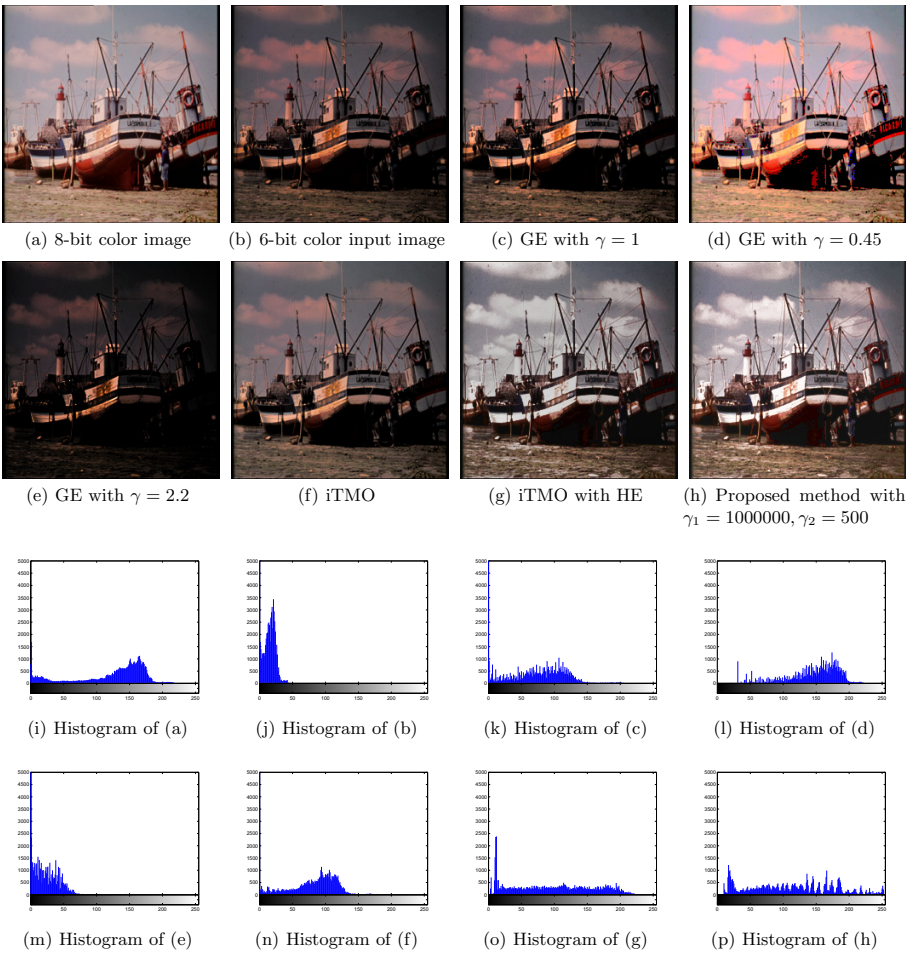

(a) 8-bit color image (b) 6-bit color input image (c) GE with $\gamma = 1$ (d) GE with $\gamma = 0.45$

(e) GE with $\gamma = 2.2$ (f) iTMO (g) iTMO with HE (h) Proposed method with $\gamma_1 = 1000000, \gamma_2 = 500$

(i) Histogram of (a) (j) Histogram of (b) (k) Histogram of (c) (l) Histogram of (d)

(m) Histogram of (e) (n) Histogram of (f) (o) Histogram of (g) (p) Histogram of (h)

Fig. 3. The Comparison of different methods for the "Boats" image

5(a) are not biased toward the small or large values. Therefore, we manually adjust their pixel values to under-exposed images (see Figures 2-3(b) and 2-3(i)) and the over-exposed images (Figures 4-5(b) and 4-5(i)).

We compare our results with Gamma expansion (GE) method [2] and Banterle's inverse tone mapping operators (iTMO) method [11]. GE method has the effect of adjusting the contrast and iTMO method simulates the camera response function. To keep comparison fair, we also consider doing the histogram equalization to the input images first and then applying iTMO method. The PSNR values between the resulting image and the original 8-bit image are shown in Table 1 except for Figure 1 where it is a low contrast image already.

The parameters in GE method is set as the same in Akyuz's psychophysical investigations in [2] with three gamma alternatives $\gamma = 1, 0.45, 2.2$. The iTMO method inverts the Reinhard's tone mapping operators in [12]. The initial local

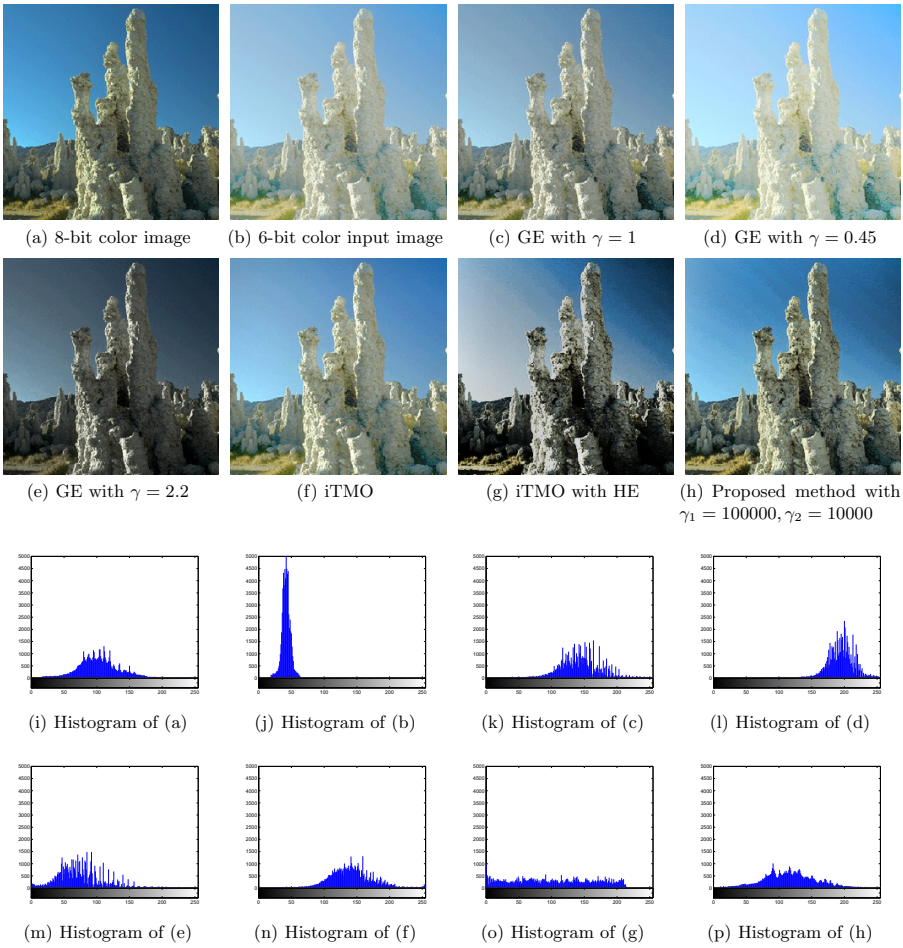

(a) 8-bit color image (b) 6-bit color input image (c) GE with $\gamma = 1$ (d) GE with $\gamma = 0.45$

(e) GE with $\gamma = 2.2$ (f) iTMO (g) iTMO with HE (h) Proposed method with $\gamma_1 = 100000, \gamma_2 = 10000$

(i) Histogram of (a) (j) Histogram of (b) (k) Histogram of (c) (l) Histogram of (d)

(m) Histogram of (e) (n) Histogram of (f) (o) Histogram of (g) (p) Histogram of (h)

Fig. 4. The Comparison of different methods for the "Monolake" image

histogram $h_{i,j}$ in equation (4) was obtained by calculating the local histograms of the input low contrast image and then linearly project them onto the desired dynamic range with zeros padding. The values of parameters β, γ_1 and γ_2 are tuned according to the PSNR values between the displayed image and the original 8-bit image. In the tests, we set the fixed value of the penalty parameter β to be 100 in the ADMM method. The stopping criterion of the ADMM method is that the relative difference between the successive iterates ϵ is less than 1×10^{-4}.

According to Figures 1-5, it can be shown from the results that the proposed method achieves better visual appearance and obtain higher PSNR values than the other testing methods in most cases. The local contrast is enhanced to increase detailed visibility. In the meanwhile, the over-exposed or under-exposed images can be adjusted through the histogram redistribution process to achieve a observer-friendly display in high bit-depth setting. These results are also re-

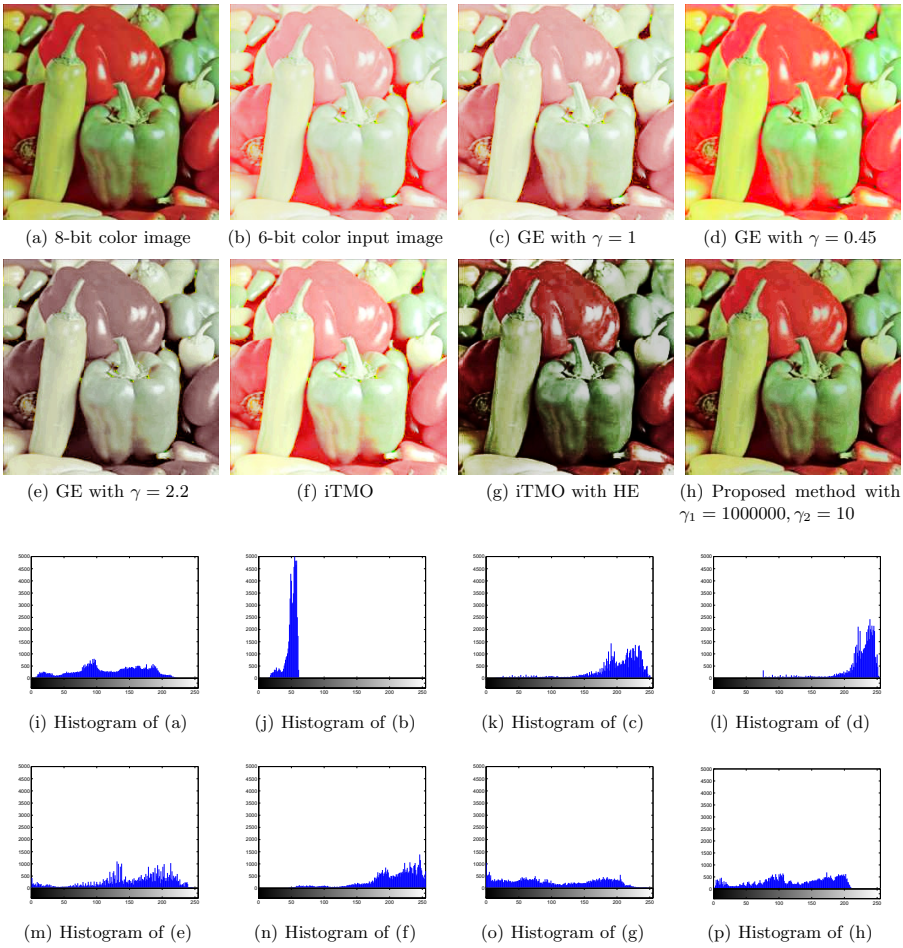

(a) 8-bit color image (b) 6-bit color input image (c) GE with $\gamma = 1$ (d) GE with $\gamma = 0.45$

(e) GE with $\gamma = 2.2$ (f) iTMO (g) iTMO with HE (h) Proposed method with $\gamma_1 = 1000000, \gamma_2 = 10$

(i) Histogram of (a) (j) Histogram of (b) (k) Histogram of (c) (l) Histogram of (d)

(m) Histogram of (e) (n) Histogram of (f) (o) Histogram of (g) (p) Histogram of (h)

Fig. 5. The Comparison of different methods for the "Peppers" image

flected from the more equalized histograms generated by the proposed method, see Figures 1-5(n). However, the histograms generated by the other methods are still biased toward either small or large pixel values, see Figures 1-5(j), 1-5(k), 1-5(l), and 1-5(m). Indeed, the results by iTMO show that the contrast can also be enhanced but only on the limited middle range. Since it only reverts by using one nonlinear *s*-shaped camera response function. it cannot deal with the regions with small or large pixel values, especially when the input image is under-exposed or over-exposed. The GE method can also control the contrast uniformly, but it cannot improve local contrast of input images.

Finally, we report the ADMM method converges very fast. In our examples, it takes around 5-10 iterations to obtain the resulting high bit-depth image, and

the computational time is about 15 seconds in average. Since we are doing local histogram calculation, the algorithm is easy to be modified to parallel computing for acceleration.

5 Concluding Remarks

In this paper, we have presented a variational method to generate a high bit-depth image from a single low bit-depth image so that it can be appropriately displayed on a high bit-depth monitor or projector. The pixel values from a low bit-depth image are mapped to that on a high bit-depth image by spatial variant mapping functions, derived from the constrained variational histogram equalization method. The energy minimization problem can be solved efficiently by ADMM algorithm. From the experimental results, we can see that the detailed visibility can be enhanced as well as avoiding the over-enhancement of the noise and other artifacts. The proposed method can also deal with the under-exposed or over-exposed input images to enhance their local contrast in the resulting high bit-depth image.

References

1. Ulichney, R., Cheung, S.: Pixel Bit-Depth Increase by Bit Replication. Color Imaging: Device-Independent Color, Color Hardcopy, and Graphic Arts III, Proceeding of SPIE, pp. 232–241 (1998)
2. Akyüz, A.O., Fleming, R., Riecke, B.E., Reinhard, E., Bülthoff, H.H.: Do HDR displays support LDR content?: a psychophysical evaluation. ACM Transactions on Graphics (TOG) 26(3), 38 (2007)
3. Robertson, M.A., Borman, S., Stevenson, R.L.: Dynamic Range Improvement through Multiple Exposures. In: Proceedings of International Conference on Image Processing, vol. 3, pp. 159–163 (1999)
4. Debevec, P.E., Malik, J.: Recovering High Dynamic Range Radiance Maps from Photographs. ACM SIGGRAPH, classes. 31 (2008)
5. Kao, W.-C.: High Dynamic Range Imaging by Fusing Multiple Raw Images and Tone Reproduction. IEEE Transactions on Consumer Electronics 54(1), 10–15 (2008)
6. Grossberg, M.D., Nayar, S.K.: High Dynamic Range from Multiple Images: Which Exposures to Combine? In: Proceedings of ICCV Workshop on Color and Photometric Methods in Computer Vision (2003)
7. Liu, C.-H., Au, O.C., Wong, P.H.W., Kung, M.C., Chao, S.-C.: Bit-Depth Expansion by Adaptive Filter. In: IEEE Inernational Symposium on Circuits and Systems, pp. 496–499 (2008)
8. Taguchi, A., Nishiyama, J.: Bit-Length Expansion by Inverse Quantization Process. In: Proceedings of the 20th European Signal Processing Conference (EUSIPCO), pp. 1543–1547 (2012)
9. Jongseong, C., Min Kyu, P., Moon Gi, K.: High Dynamic Range Image Reconstruction with Spatial Resolution Enhancement. The Computer Journal 52(1), 114–125 (2009)

10. Altas, I., Louis, J., Belward, J.: A Variational Approach to the Radiometric Enhancement of Digital Imagery. IEEE Transactions on Image Processing 4(6), 845–849 (1995)
11. Banterle, F., Ledda, P., Debattista, K., Chalmers, A.: Inverse Tone Mapping. In: Proceedings of 4th International Conference on Computer Graphics and Interactive Techniques in Australisia and Southeast Asia, pp. 349–356 (2006)
12. Reinhard, E., Stark, M., Shirley, P., Ferwerda, J.: Photographic Tone Reproduction for Digital Images. ACM Transactions on Graphics 21(3), 267–276 (2002)